2008 American Control Conference
Westin Seattle Hotel, Seattle, Washington, USA
June 11-13, 2008

Coverage control by robotic networks with limited-range anisotropic sensory

Katie Laventall and Jorge Cortés

Abstract— **This paper considers the deployment of a network of robotic agents with limited-range communication and anisotropic sensing capabilities. We encode the environment coverage provided by the network by means of an expected-value objective function. This function has a gradient which is not amenable to distributed computation. We provide a constant-factor approximation of this measure via an alternative aggregate objective function whose gradient is spatially distributed over the limited-range Delaunay proximity graph. We characterize the smoothness properties of the aggregate expected-value function and propose a distributed deployment algorithm to optimize it. Simulations illustrate the results.**

I. Introduction

Currently there is a large interest in the design of stable and decentralized control laws for distributed motion coordination. In this paper, we focus on the deployment of a robotic network where each agent is equipped with limited-range communication and anisotropic sensing capabilities (e.g., cameras). We model the restricted sensory range by defining a wedge-shaped region centered about each robot's orientation with an angular width less than or equal to π radians. Our objective is to design distributed coordination algorithms that optimize sensor network coverage of a convex closed environment.

The literature on coordination tasks for robotic systems is becoming quite extensive. The deployment problem considered here falls within the field of facility location [1], [2], [3], where one seeks to optimize the position of a number of resources in order to provide better quality-of-service. In particular, this paper builds on [4], which provides an overview of coverage control for mobile networks, and [5], which models systems with limited-range interactions. Other works on coverage problems include [6], [7], [8], [9]. Our technical approach uses concepts and notions from computational geometry and geometric optimization, such as Voronoi partitions [1], proximity graphs [10], and spatially distributed maps [5].

The contributions of the paper are threefold. First, we define a novel proximity graph, termed the limited-range wedge graph, and show that it is distributed over the limited-range Delaunay graph. Second, we introduce the *expected-value* locational optimization function to measure the network coverage of the environment. Motivated by the fact that the gradient of this function is not amenable to distributed computation, we provide a constant-factor approximation via an alternative *aggregate expected-value* objective function. We characterize the smoothness properties of the aggregate expected-value function and show that the limited-range wedge graph plays a key role in the computation of its gradient. As an important consequence, we show that the gradient is spatially distributed over the limited-range Delaunay graph. Third, we propose a distributed gradient ascent algorithm to optimize network coverage and provide simulations to illustrate the algorithm execution.

The organization of this paper is as follows. Section II presents useful concepts on Voronoi partitions, proximity graphs, and spatially distributed maps. Section III introduces the expected-value and aggregate expected-value functions, discusses a constant-factor approximation between them, and analyzes their distributed character. Based on these results, Section IV presents a deployment algorithm spatially distributed over the limited-range Delaunay graph and illustrates it in simulation. Section V gathers our conclusions and ideas for future work.

II. Preliminary developments

In this section we present various notational conventions and discuss notions from computational geometry. Let $\mathbb{R}$, $\mathbb{R}_{>0}$, and $\mathbb{R}_{\geq 0}$ be the set of real, positive real, and non-negative real numbers. Let $\mathbb{F}(\mathbb{R}^d)$ be the set of all finite pointsets in $\mathbb{R}^d$. For $x \in \mathbb{R}^d$, let $x^{\mathbf{T}}$ denote the transpose of x. Given a set S in $\mathbb{R}^d$, let $\mathrm{co}(S)$ and $\mathrm{int}(S)$ be the convex hull and the interior of S, respectively. The *indicator function* $1_S : \mathbb{R}^d \to \mathbb{R}$ of the set S is defined by $1_S(q) = 1$ if $q \in S$ and $1_S(q) = 0$ if $q \notin S$. For an integrable function $\phi : \mathbb{R}^d \to \mathbb{R}_{\geq 0}$, let $\mathrm{area}_\phi(S) = \int_S \phi(x)dx$. Let $\overline{B}(x, r)$ denote the closed ball centered at x with radius r, and $\mathrm{arc}(x, r)$ denote an arc segment of $\partial\overline{B}(x, r)$. Throughout the paper, $Q \subset \mathbb{R}^2$ denotes a simple convex polygon. The *diameter* of Q is $\mathrm{diam}(Q) = \max_{q,p\in Q} \|q - p\|$. Lastly, we define the unit vector $u_\theta = [\cos\theta, \sin\theta]^{\mathbf{T}}$ and the counterclockwise rotation-by-θ-radians matrix

$$\mathrm{Rot}_\theta = \begin{pmatrix} \cos\theta & -\sin\theta \\ \sin\theta & \cos\theta \end{pmatrix}.$$

A. Voronoi partitions and boundary parameterizations

Voronoi partitions can be defined in arbitrary metric spaces, but here we restrict our attention to the plane. The *Voronoi partition* generated by $\mathcal{P} = \{p_1, \ldots, p_n\} \subset \mathbb{R}^2$ is the collection $\mathcal{V}(\mathcal{P}) = (V_1(\mathcal{P}), \ldots, V_n(\mathcal{P}))$ where,

$$V_i(\mathcal{P}) = \{q \in \mathbb{R}^2 \mid \|q - p_i\| \leq \|q - p_j\|, \text{ for all } p_j \in \mathcal{P}\}.$$

Often, we use the notation V_i instead of $V_i(\mathcal{P})$. Two robots i and j are Voronoi neighbors if $V_i \cap V_j \neq \emptyset$. The section of the boundary of $V_i(\mathcal{P})$ that corresponds to the intersection with $V_j(\mathcal{P})$ is counterclockwise parametrized as

$$\gamma_{ij}(t) = \frac{p_i + p_j}{2} + t\,\mathrm{Rot}_{\frac{\pi}{2}}(p_j - p_i), \quad t \in [c_i, d_i], \qquad (1)$$

for some $c_i, d_i \in \mathbb{R}$. The corresponding outward unit normal vector is $n_{ij} = \frac{p_j - p_i}{\|p_j - p_i\|}$, see Fig. 1.

Katie Laventall is with the Aeronautics and Astronautics Department, Stanford University, Stanford, CA 94305, klaventall@stanford.edu
Jorge Cortés is with the Department of Mechanical and Aerospace Engineering, University of California, San Diego, CA 92093, cortes@ucsd.edu

978-1-4244-2079-7/08/$25.00 ©2008 AACC.

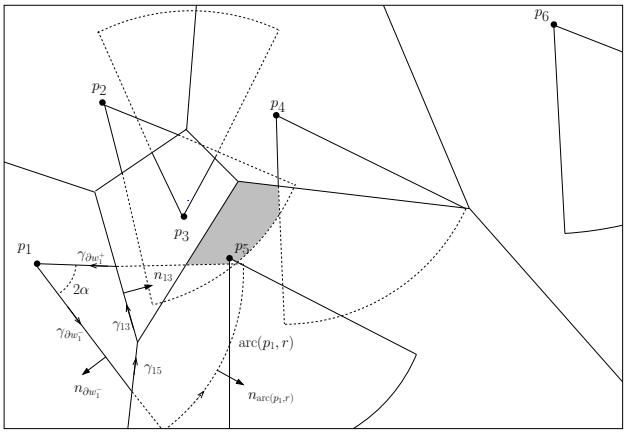

Fig. 1. Voronoi partition and wedge-shaped sensing regions corresponding to a random deployment of a robotic network. The parameters are $\alpha = \frac{\pi}{8}$ and $r = 0.5$. The notation for the various parameterizations of the Voronoi cell boundary and wedge sensing region are specified for robot 1.

The Voronoi partition of an ordered set of possibly coincident points is not well-defined. To deal with this situation, we introduce the immersion $i_{\mathbb{F}} : (\mathbb{R}^2)^n \to \mathbb{F}(\mathbb{R}^2)$ that maps P to the pointset $\mathcal{P}$ containing the distinct points in P. The cardinality of $\mathcal{P}$ is determined by whether P is an element of the set

$$\mathcal{S}_{\text{coinc}} = \{(p_1, \ldots, p_n) \in (\mathbb{R}^d)^n \mid p_i = p_j \text{ for some } i \neq j \in \{1, \ldots, n\}\}. \quad (2)$$

For $P \in \mathcal{S}_{\text{coinc}}$, we consider the Voronoi partition generated by $\mathcal{P} = i_{\mathbb{F}}(P)$.

B. Limited-range anisotropic sensory

Let $P = (p_1, \ldots, p_n) \in Q^n$ be a tuple of points in Q, where p_i is the position of robot i, and let $\Theta = (\theta_1, \ldots, \theta_n) \in (\mathbb{S}^1)^n$ be a tuple of angles, where θ_i is the orientation of robot i. For $P \in Q^n$ and $\Theta \in (\mathbb{S}^1)^n$, we denote $((p_1, \theta_1), \ldots, (p_n, \theta_n)) \in (\mathbb{R}^2 \times \mathbb{S}^1)^n$ by (P, Θ) with a slight abuse of notation. We define the wedge-shaped sensory region $w_{r,\alpha}(p, \theta)$ as the sector of a circle of radius r, centered at p, with orientation θ, and amplitude 2α, $\alpha \in (0, \frac{\pi}{2}]$, see Fig. 1. For brevity, we occasionally denote the region $w_{r,\alpha}(p_i, \theta_i)$ of robot i by w_i. The indicator function of the region $w_{r,\alpha}(p, \theta)$ can be expressed by

$$1_{w_{r,\alpha}(p,\theta)}(q) = \begin{cases} 1, & \text{if } \|q - p\| \leq r \text{ and} \\ & \arccos\left(\frac{|(q-p)\cdot(\cos\theta, \sin\theta)|}{\|q-p\|}\right) \leq \alpha, \\ 0, & \text{otherwise.} \end{cases}$$

It is convenient to decompose the boundary $\partial w_{r,\alpha}(p, \theta)$ of the wedge into the union of two line segments ∂w^+, ∂w^- and an arc segment $\mathrm{arc}(p, r)$. We consider the following counterclockwise parametrization of $\partial w_{r,\alpha}(p, \theta)$,

$$\gamma_{\partial w^-}(t) = p + t u_{\theta-\alpha}, \qquad t \in [0, r], \quad (3a)$$
$$\gamma_{\mathrm{arc}(p,r)}(t) = p + r u_{\theta+t}, \qquad t \in [-\alpha, \alpha], \quad (3b)$$
$$\gamma_{\partial w^+}(t) = p + (r - t) u_{\theta+\alpha}, \quad t \in [0, r]. \quad (3c)$$

The corresponding outward normal vectors are

$$n_{\partial w^-}(q) = \mathrm{Rot}_{\frac{-\pi}{2}}\, u_{\theta-\alpha}, \qquad q \in \partial w^-, \quad (4a)$$
$$n_{\mathrm{arc}(p,r)}(q) = \frac{q - p}{\|q - p\|}, \qquad q \in \mathrm{arc}(p, r), \quad (4b)$$
$$n_{\partial w^+}(q) = \mathrm{Rot}_{\frac{\pi}{2}}\, u_{\theta+\alpha}, \qquad q \in \partial w^+. \quad (4c)$$

These parameterizations are illustrated in Fig. 1.

C. Proximity graphs and spatially distributed maps

The notion of proximity graph is useful to model the changing interactions in a mobile network, see [5], [10]. A proximity graph function assigns to a pointset a graph whose vertex set is the pointset, and whose edge set is determined by the relative location of its vertices. Here we only consider proximity graphs defined for points in the plane. Let $\mathbb{G}(\mathbb{R}^2)$ be the set of directed graphs whose vertex set is an element of $\mathbb{F}(\mathbb{R}^2)$. A *proximity graph function* $\mathcal{G} : \mathbb{F}(\mathbb{R}^2) \to \mathbb{G}(\mathbb{R}^2)$ associates to $\mathcal{V} \in \mathbb{F}(\mathbb{R}^2)$ a graph with vertex set $\mathcal{V}$ and edge set $\mathcal{E}_{\mathcal{G}}(\mathcal{V})$, where $\mathcal{E}_{\mathcal{G}} : \mathbb{F}(\mathbb{R}^2) \to \mathbb{F}(\mathbb{R}^2 \times \mathbb{R}^2)$ has the property that $\mathcal{E}_{\mathcal{G}}(\mathcal{V}) \subseteq \mathcal{V} \times \mathcal{V} \setminus \mathrm{diag}(\mathcal{V} \times \mathcal{V})$. The following proximity graph functions are relevant to our discussion:

(i) the *r-disk graph* $\mathcal{P} \mapsto \mathcal{G}_{\text{disk}}(\mathcal{P}, r) = (\mathcal{P}, \mathcal{E}_{\mathcal{G}_{\text{disk}}}(\mathcal{P}, r))$, with

$$\mathcal{E}_{\mathcal{G}_{\text{disk}}}(\mathcal{P}, r) = \{(p_i, p_j) \in \mathcal{P} \times \mathcal{P} \setminus \mathrm{diag}(\mathcal{P} \times \mathcal{P}) \mid \|p_i - p_j\| \leq r\};$$

(ii) the *Delaunay graph* $\mathcal{P} \mapsto \mathcal{G}_D(\mathcal{P}) = (\mathcal{P}, \mathcal{E}_{\mathcal{G}_D}(\mathcal{P}))$, with

$$\mathcal{E}_{\mathcal{G}_{\text{D}}}(\mathcal{P}) = \{p_i, p_j \in \mathcal{P} \times \mathcal{P} \setminus \mathrm{diag}(\mathcal{P} \times \mathcal{P}) \mid V_i \cap V_j \neq \emptyset\};$$

(iii) the *r-limited (or limited-range) Delaunay graph* $\mathcal{P} \mapsto \mathcal{G}_{\text{LD}}(\mathcal{P}, r) = (\mathcal{P}, \mathcal{E}_{\mathcal{G}_{\text{LD}}}(\mathcal{P}, r))$, with edges $(p_i, p_j) \in \mathcal{P} \times \mathcal{P} \setminus \mathrm{diag}(\mathcal{P} \times \mathcal{P})$ if

$$\big(V_i(\mathcal{P}) \cap \overline{B}(p_i, \tfrac{r}{2})\big) \cap \big(V_j(\mathcal{P}) \cap \overline{B}(p_j, \tfrac{r}{2})\big) \neq \emptyset;$$

(iv) the *(r, α)-limited (or limited-range) wedge graph* $(\mathcal{P}, \Theta) \mapsto \mathcal{G}_{\text{LW}}(\mathcal{P}, \Theta) = (\mathcal{P}, \mathcal{E}_{\mathcal{G}_{\text{LW}}}(\mathcal{P}, \Theta))$, with edges $((p_i, \theta_i), (p_j, \theta_j)) \in (\mathcal{P}, \Theta) \times (\mathcal{P}, \Theta)$ if

$$\big(V_i(\mathcal{P}) \cap V_j(\mathcal{P})\big) \cap w_{\frac{r}{2},\alpha}(p_i, \theta_i) \neq \emptyset.$$

Fig. 2 presents an illustration of these notions. Note that the orientation of the robots does not affect the computation of the r-limited Delaunay graph. The r-limited Delaunay graph is undirected, whereas the (r, α)-limited wedge graph is directed. Clearly it is possible for $V_i \cap V_j \cap w_{r,\alpha}(p_i, \theta_i) \neq \emptyset$ and $V_i \cap V_j \cap w_{r,\alpha}(p_j, \theta_j) = \emptyset$ simultaneously, see for instance Fig. 1.

For a directed proximity graph $\mathcal{G}$, q is an *in-neighbor* of v (or equivalently v is an *out-neighbor* of q) if $(q, v) \in \mathcal{E}_{\mathcal{G}}(\mathcal{V})$. To a vertex v, one can associate the set of *in-neighbors* and *out-neighbors* maps $\mathcal{N}^{in}_{\mathcal{G},v}, \mathcal{N}^{\text{out}}_{\mathcal{G},v} : \mathbb{F}(X) \to \mathbb{F}(X)$ defined by

$$\mathcal{N}^{\text{in}}_{\mathcal{G},v}(\mathcal{V}) = \{q \in \mathcal{V} \mid (q, v) \in \mathcal{E}_{\mathcal{G}}(\mathcal{V} \cup \{v\})\},$$
$$\mathcal{N}^{\text{out}}_{\mathcal{G},v}(\mathcal{V}) = \{q \in \mathcal{V} \mid (v, q) \in \mathcal{E}_{\mathcal{G}}(\mathcal{V} \cup \{v\})\}.$$

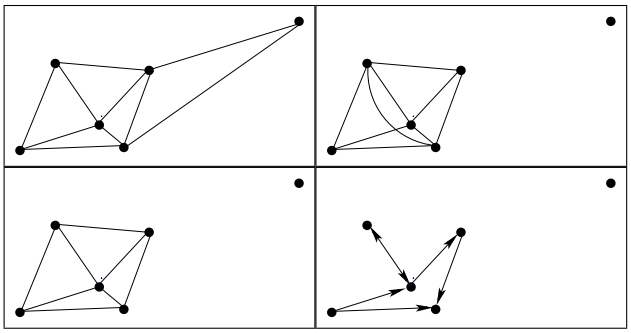

Fig. 2. From left to right, Delaunay graph, r-disk graph, r-limited Delaunay graph, and (r,α)-limited wedge graph corresponding to the configuration in Fig. 1. The parameters are $\alpha = \frac{\pi}{8}$ and $r = 0.5$.

A proximity graph $\mathcal{G}_1$ is *spatially distributed* over an undirected proximity graph $\mathcal{G}_2$ if, for all $\mathcal{V} \in \mathbb{F}(X)$ and all $v \in \mathcal{V}$, we have

$$\mathcal{N}^{\text{in}}_{\mathcal{G}_1,v}(\mathcal{V}) = \mathcal{N}^{\text{in}}_{\mathcal{G}_1,v}(\mathcal{N}_{\mathcal{G}_2,v}(\mathcal{V})),$$
$$\mathcal{N}^{\text{out}}_{\mathcal{G}_1,v}(\mathcal{V}) = \mathcal{N}^{\text{out}}_{\mathcal{G}_1,v}(\mathcal{N}_{\mathcal{G}_2,v}(\mathcal{V})).$$

The next result establishes that the limited-range wedge graph is spatially distributed over the limited-range Delaunay graph.

Lemma II.1 *The (r,α)-limited wedge graph $\mathcal{G}_{\text{LW}}$ is spatially distributed over the r-limited Delaunay graph $\mathcal{G}_{\text{LD}}$.*

Proof: Note that $V_i(\mathcal{P}) \cap V_j(\mathcal{P}) \cap w_{\frac{r}{2},\alpha}(p_i,\theta_i) \neq \emptyset$ implies that $\overline{B}(p_i,\frac{r}{2}) \cap \{q \in \mathbb{R}^2 \mid \|q-p_i\| = \|q-p_j\|\} \neq \emptyset$. The latter is equivalent to $\overline{B}(p_j,\frac{r}{2}) \cap \{q \in \mathbb{R}^2 \mid \|q-p_i\| = \|q-p_j\|\} \neq \emptyset$. Therefore,

$$\begin{aligned}
&\mathcal{N}^{\text{out}}_{\mathcal{G}_{\text{LW}},(p_i,\theta_i)}(\mathcal{P},\Theta)\\
&= \{(p_j,\theta_j) \in (\mathcal{P},\Theta) \mid V_i(\mathcal{P}) \cap V_j(\mathcal{P}) \cap w_{\frac{r}{2},\alpha}(p_i,\theta_i) \neq \emptyset\}\\
&= \{(p_j,\theta_j) \in \mathcal{N}_{\mathcal{G}_{\text{LD}},(p_i,\theta_i)}(\mathcal{P},\Theta) \mid\\
&\qquad\qquad V_i(\mathcal{P}) \cap V_j(\mathcal{P}) \cap w_{\frac{r}{2},\alpha}(p_i,\theta_i) \neq \emptyset\}\\
&= \mathcal{N}^{\text{out}}_{\mathcal{G}_{\text{LW}},(p_i,\theta_i)}(\mathcal{N}_{\mathcal{G}_{\text{LD}},(p_i,\theta_i)}(\mathcal{P},\Theta)).
\end{aligned}$$

A similar proof can be given for $\mathcal{N}^{\text{in}}_{\mathcal{G}_{\text{LW}},(p_i,\theta_i)}(\mathcal{P},\Theta)$. ■

III. Encoding network performance via locational optimization

We begin by introducing measures of the sensor coverage of the environment by the robotic network.

A. Expected-value locational optimization functions

Let $\phi : Q \to \mathbb{R}_{\geq 0}$ be an integrable *density* function. This function can be thought of as a measure of the probability of some event taking place over Q. Due to noise and interference, the sensor performance of robot i degrades at point q in proportion to the distance $\|q-p_i\|$. Thus, we introduce a continuously differentiable, strictly positive, non-increasing *performance* function $f : \mathbb{R}_{\geq 0} \to \mathbb{R}_{\geq 0}$ to measure this degradation: $f(\|q-p_i\|)$ provides a quantitative assessment of sensor quality of the ith robot at point $q \in Q$. Consider then the *expected-value* locational optimization function $\mathcal{H} : (Q \times \mathbb{S}^1)^n \to \mathbb{R}_{\geq 0}$,

$$\mathcal{H}(P,\Theta) = \int_Q \max_{i\in\{1,\dots,n\}} \left\{f(\|q-p_i\|)1_{w_{r,\alpha}(p_i,\theta_i)}(q)\right\}\phi(q)dq. \tag{5}$$

This function provides an expected value of the sensor network performance. Hence, it is of interest to find maximizers of $\mathcal{H}$. However, its gradient is in general not distributed over the limited-range Delaunay or limited-range wedge graphs. Fig. 1 illustrates this assertion. The sensing region of p_2 is the only one that contains the grey region depicted in the plot. Changes in p_5 affect the gradient of $\mathcal{H}$ with respect to p_2. However, p_2 and p_5 are not neighbors in the limited-range Delaunay or limited-range wedge graphs.

The approach we take here is to provide an alternative objective function. We define the *aggregate expected-value* locational optimization function

$$\mathcal{H}_{\text{agg}}(P,\Theta) = \int_Q \max_{i\in\{1,\dots,n\}} \left\{f(\|q-p_i\|)\right\} 1_{\cup_{p_j\in M(q)} w_{r,\alpha}(p_j,\theta_j)}(q)\phi(q)dq, \tag{6}$$

where $M(q) = \text{argmin}\{\|q-p_i\|\}$. For $P \notin \mathcal{S}_{\text{coinc}}$, the function $\mathcal{H}_{\text{agg}}$ can be rewritten as

$$\mathcal{H}_{\text{agg}}(P,\Theta) = \sum_{i=1}^n \int_{V_i(P)} f(\|q-p_i\|)1_{w_{r,\alpha}(p_i,\theta_i)}(q)\phi(q)dq. \tag{7}$$

The function $\mathcal{H}_{\text{agg}}$ sums the individual sensor performance of the robots within the intersection of their respective sensing wedge and Voronoi cell. Note that the function is discontinuous at coincident configurations. Let us show that $\mathcal{H}_{\text{agg}}$ provides a good approximation of $\mathcal{H}$ on suitable regions of the configuration space $(Q \times \mathbb{S}^1)^n$.

Proposition III.1 *Consider the expected-value and aggregate expected-value objective functions, $\mathcal{H}$ and $\mathcal{H}_{agg}$ respectively. Then, for all $(P,\Theta) \in (Q \times \mathbb{S}^1)^n$,*

$$\mathcal{H}_{agg}(P,\Theta) \leq \mathcal{H}(P,\Theta) \leq \mathcal{H}_{agg}(P,\Theta) + \|f\|_\infty \,\text{area}_\phi(Q),$$

where $\|f\|_\infty = \max_{x\in[0,\text{diam}\,Q]} |f(x)|$. Additionally, for $A \in (0,\text{area}_\phi(Q)]$, define

$$\begin{aligned}
\Sigma_A =&\{(P,\Theta) \in (Q \times \mathbb{S}^1)^n\\
&\mid \sum_{j=1}^m \text{area}_\phi(V_j(i_{\mathbb{F}}(P)) \cap (\cup_{\substack{i \text{ s.t.}\\ p_i=z_j}} w_{r,\alpha}(p_i,\theta_i))) \geq A\},
\end{aligned}$$

where recall $i_{\mathbb{F}}(P) = \{z_1,\dots,z_m\}$. Then, for all $(P,\Theta) \in \Sigma_A$,

$$\mathcal{H}_{agg}(P,\Theta) \leq \mathcal{H}(P,\Theta) \leq \Big(1 + \frac{\|f\|_\infty \,\text{area}_\phi(Q)}{A\, f(\text{diam}(Q))}\Big)\mathcal{H}_{agg}(P,\Theta).$$

Proof: The lower bounds in both approximations follow directly from the function definition in (5) and (6). For $P \notin \mathcal{S}_{\text{coinc}}$, the upper bound in the additive approximation follows

from

$$\begin{aligned}
&\mathcal{H}(P,\Theta) - \mathcal{H}_{\text{agg}}(P,\Theta) \\
&\quad \le \sum_{i=1}^{n} \int_{V_i} f(\|q-p_i\|) \\
&\qquad \big(\max_{j\in\{1,\dots,n\}} \{1_{w_{r,\alpha}(p_j,\theta_j)}(q)\} - 1_{w_{r,\alpha}(p_i,\theta_i)}(q) \big) \phi(q) dq \\
&\quad \le \sum_{i=1}^{n} \int_{V_i \cap Q \setminus w_{r,\alpha}(p_i,\theta_i)} f(\|q-p_i\|)\phi(q)dq \\
&\quad \le \|f\|_\infty \operatorname{area}_\phi(Q \setminus \cup_{i=1}^{n} w_{r,\alpha}(p_i,\theta_i)) \\
&\quad \le \|f\|_\infty \operatorname{area}_\phi(Q).
\end{aligned}$$

A similar set of inequalities can be derived for $P \in \mathcal{S}_{\text{coinc}}$. The upper bound in the constant-factor approximation follows from the above upper bound and the fact that

$$\begin{aligned}
&\mathcal{H}_{\text{agg}}(P,\Theta) \\
&\ge f(\operatorname{diam}(Q)) \sum_{j=1}^{m} \operatorname{area}_\phi(V_j(i_{\mathbb{F}}(P)) \cap (\cup_{\substack{i \text{ s.t.} \\ p_i = z_j}} w_{r,\alpha}(p_i,\theta_i))) \\
&\ge A\, f(\operatorname{diam}(Q))
\end{aligned}$$

on Σ_A. ■

From Proposition III.1, one can see that the better the area coverage of Q provided by the collection of sets resulting from the intersection between Voronoi regions and wedges, the better the approximation of $\mathcal{H}$ provided by $\mathcal{H}_{\text{agg}}$ is. From (6), configurations with larger values of $\mathcal{H}_{\text{agg}}$ also induce good area coverage of Q. Therefore, the maximization of $\mathcal{H}_{\text{agg}}$ naturally leads to regions of good approximations of $\mathcal{H}$.

Remark III.2 For $P \in Q^n$ such that $\|z_i - z_j\| > 2r$, for all $z_i, z_j \in i_{\mathbb{F}}(P)$, the values of $\mathcal{H}$ and $\mathcal{H}_{\text{agg}}$ coincide, i.e., $\mathcal{H}(P,\Theta) = \mathcal{H}_{\text{agg}}(P,\Theta)$, for all $\Theta \in (\mathbb{S}^1)^n$. •

B. Smoothness properties of the aggregate expected-value function

We explore the smoothness properties of the function $\mathcal{H}_{\text{agg}}$.

Theorem III.3 *Given a density function ϕ and a performance function f, the function $\mathcal{H}_{agg}$ is piecewise continuously differentiable. On $\mathcal{S}_{coinc}$, $\mathcal{H}_{agg}$ is discontinuous. On $\operatorname{int}(Q)^n \setminus \mathcal{S}_{coinc}$, $\mathcal{H}_{agg}$ is continuously differentiable and, for each $i \in \{1,\dots,n\}$, its gradient is given by*

$$\begin{aligned}
\frac{\partial \mathcal{H}_{agg}}{\partial p_i} &= \int_{V_i \cap w_i} \frac{\partial}{\partial p_i} f(\|q-p_i\|)\phi(q)dq \qquad (8a) \\
&+ \int_{V_i \cap (\partial w_i^+ \cup \partial w_i^-)} f(\|q-p_i\|)\phi(q)n(q)dq \\
&+ \int_{V_i \cap w_i \cap \partial \overline{B}(p_i,r)} f(\|q-p_i\|)\phi(q)n(q)dq \\
&+ \sum_{\substack{j=1 \\ j\neq i}}^{n} \Big(\int_{V_i \cap V_j \cap w_i} f(\|q-p_i\|)\phi(q) \frac{q-p_i}{\|p_j-p_i\|} dq \\
&- \int_{V_i \cap V_j \cap w_j} f(\|q-p_j\|)\phi(q) \frac{q-p_i}{\|p_j-p_i\|} dq \Big),
\end{aligned}$$

where $n(q)$ denotes the unit outward normal vector at q, and

$$\frac{\partial \mathcal{H}_{agg}}{\partial \theta_i} = \sum_{s\in\{+,-\}} s \int_{V \cap \partial w_i^s} \|q-p_i\| f(\|q-p_i\|)\phi(q)dq. \qquad (8b)$$

Proof: For $P \in \operatorname{int}(Q)^n \setminus \mathcal{S}_{\text{coinc}}$, consider the expression (7) of $\mathcal{H}_{\text{agg}}$. Note that $f(\|q-p_i\|)$ is continuously differentiable and for fixed (P,Θ), the maps $q \mapsto f(\|q-p_i\|)$ and $q \mapsto \frac{\partial}{\partial P} f(\|q-p_i\|)$ are both measurable and integrable on $V_i \cap w_{r,\alpha}(p_i,\theta_i)$. Also note that since both the Voronoi partition and the wedge are convex sets, their intersection is also convex. By [5, Proposition A.1] (see also Appendix A), $\mathcal{H}_{\text{agg}}$ is continuously differentiable on $(\operatorname{int}(Q)^n \setminus \mathcal{S}_{\text{coinc}}) \times (\mathbb{S}^1)^n$ and, for each $i \in \{1,\dots,n\}$,

$$\begin{aligned}
\frac{\partial \mathcal{H}_{\text{agg}}}{\partial p_i}(P,\Theta) &= \frac{\partial}{\partial p_i} \sum_{k=1}^{n} \int_{V_k \cap w_k} f(\|q-p_k\|)\phi(q)dq \qquad (9) \\
&= \int_{V_i \cap w_i} \frac{\partial}{\partial p_i} f(\|q-p_k\|)\phi(q)dq \\
&+ \sum_{k=1}^{n} \int_{\partial(V_k \cap w_k)} f(\|\gamma-p_k\|)\phi(\gamma) n^{\mathbf{T}}(\gamma) \frac{\partial \gamma}{\partial p_i} d\gamma.
\end{aligned}$$

Next, we simplify the second term in the equation. The boundary $\partial(V_k \cap w_{r,\alpha}(p_k,\theta_k))$ is composed of a finite number of line segments and arcs, all of which have been parametrized in Section II-A. We first integrate over the wedge boundary $V_k \cap \partial(w_{r,\alpha}(p_k,\theta_k)) = V_k \cap (\partial w_k^+ \cup \partial w_k^-) \cup_{l=1}^{m} \operatorname{arc}_l(p_k,r)$, see (3). This integral is nonzero only when $k=i$. Note that when there is a displacement in the position of p_i, the motion of $w_{r,\alpha}(p_i,\theta_i)$ (when projected along the appropriate normal vector) is exactly the same as p_i i.e., $n_{(\cdot)}^{\mathbf{T}} \frac{\partial \gamma_{(\cdot)}}{\partial p_i} = n_{(\cdot)}$. Hence,

$$\begin{aligned}
&\int_{V_i \cap (\partial w_k^+ \cup \partial w_k^-) \cup_{l=1}^{m} \operatorname{arc}(p_i,r))} f(\|q-p_i\|)\phi(q) n_{(\cdot)}^{\mathbf{T}} \frac{\partial \gamma_{(\cdot)}}{\partial p_i} d\gamma \\
&= \int_{V_i \cap (\partial w_i^+ \cup \partial w_i^-)} f(\|q-p_i\|)\phi(q) n_{\partial w_i^{(\cdot)}} dq \\
&+ \sum_{l=1}^{m} \int_{\operatorname{arc}_l(p_i,r)} f(\|q-p_i\|)\phi(q) n_{\overline{B}(p_i,r)} dq.
\end{aligned}$$

The remaining boundary segments that must be considered define the regions $V_k \cap V_j \cap w_{r,\alpha}(p_k,\theta_k)$, for $j \in \{1,\dots,n\}$. To parametrize these boundaries, consider the map given in (1). The derivative of this map with respect to p_i is non-zero only for the regions $V_i \cap V_j \cap w_{r,\alpha}(p_i,\theta_i)$ and $V_j \cap V_i \cap w_{r,\alpha}(p_j,\theta_j)$, i.e., when $p_j \in \mathcal{N}^{\text{in}}_{\mathcal{G}_{\text{LW}},(p_i,\theta_i)}(P,\Theta)$ or $p_j \in \mathcal{N}^{\text{out}}_{\mathcal{G}_{\text{LW}},(p_i,\theta_i)}(P,\Theta)$, respectively. For both regions, we use the counterclockwise parametrization γ_{ij}. When $p_j \in \mathcal{N}^{\text{in}}_{\mathcal{G}_{\text{LW}},(p_i,\theta_i)}(P,\Theta)$ we compute,

$$\begin{aligned}
n_{ij}^{\mathbf{T}} \frac{\partial \gamma_{ij}}{\partial p_i} &= \frac{1}{2} n_{ij}^{\mathbf{T}} + \frac{t}{\|p_j-p_i\|} \operatorname{Rot}_{\frac{\pi}{2}}(p_j-p_i) \\
&= \frac{1}{2} n_{ij}^{\mathbf{T}} + \frac{1}{\|p_j-p_i\|}(\gamma_{ij} - \frac{p_i+p_j}{2}) = \frac{\gamma_{ij}-p_i}{\|p_j-p_i\|}.
\end{aligned}$$

For $p_j \in \mathcal{N}^{\text{out}}_{\mathcal{G}_{\text{LW}},(p_i,\theta_i)}(P,\Theta)$, a similar computation is made using the inward normal vector $n_{ji} = -n_{ij}$. We place

these formulations back into (9) to obtain the complete form of (8a).

Next, let us compute the partial derivative of $\mathcal{H}_{\text{agg}}$ with respect to θ_i by considering the parameterizations given in (3). Since the boundary $\partial(w_{r,\alpha}(p_i,\theta_i)) \cap V_i$ contains the only parametrization with a dependency on θ_i, we have

$$\frac{\partial \mathcal{H}_{\text{agg}}}{\partial \theta_i}(P,\Theta) = \int_{\partial(w_{r,\alpha}(p_i,\theta_i))\cap V_i} f(\|\gamma - p_i\|)\phi(\gamma) n^{\mathbf{T}}(\gamma) \frac{\partial \gamma}{\partial \theta_i} d\gamma.$$

Notice that the normal vector $n_{\overline{B}(p_i,r)}$ is orthogonal to $\frac{\partial \gamma_{\text{arc}(p_i,r)}}{\partial \theta_i}$. Hence, we only consider the line segments $\partial w_i^+ \cap V_i$ and $\partial w_i^- \cap V_i$. For $q \in \partial w_i^+$ we compute,

$$n_{\partial w_i^+}^{\mathbf{T}} \frac{\partial \gamma_{\partial w_i^+}}{\partial \theta_i} = \|\gamma_{\partial w_i^+} - p_i\|.$$

Hence,

$$\int_{\partial w_i^+ \cap V_i} f(\|\gamma_{\partial w_i^+} - p_i\|)\phi(\gamma_{\partial w_i^+}) n(\gamma_{\partial w_i^+})^{\mathbf{T}} \frac{\partial \gamma_{\partial w_i^+}}{\partial \theta_i} d\gamma_{\partial w_i^+} = \int_{\partial w_i^+ \cap V_i} \|q - p_i\| f(\|q - p_i\|)\phi(q) dq.$$

A similar calculation for the integral over $\partial w_i^- \cap V_i$ completes the proof. ■

Remark III.4 Using extension by continuity, we redefine the domain where $\mathcal{H}_{\text{agg}}$ is continuously differentiable to include the boundary of Q. •

IV. A COORDINATION ALGORITHM TO OPTIMIZE NETWORK PERFORMANCE

Here we present an algorithm to maximize the locational optimization function $\mathcal{H}_{\text{agg}}$. We implement our control law in continuous time and analyze its convergence properties. Assume the robotic agents evolve according to

$$\dot{p}_i = u_i, \quad \dot{\theta}_i = v_i, \quad i \in \{1,\dots,n\}.$$

Regarding sensing, we assume that each agent has a limited-range wedge-shaped sensory region with parameters $r \in \mathbb{R}_{>0}$ and $\alpha \in (0, \frac{\pi}{2}]$. Regarding communication, we assume that each agent can share position and orientation information with other agents within a distance $2r \in \mathbb{R}_{>0}$. We implement a gradient ascent of the locational optimization function $\mathcal{H}_{\text{agg}}$. In other words, for agents not co-located with any other agent, we set

$$u_i = \begin{cases} \frac{\partial \mathcal{H}_{\text{agg}}}{\partial p_i} & p_i \in \text{int}(Q), \\ \text{pr}_Q(\frac{\partial \mathcal{H}_{\text{agg}}}{\partial p_i}) & p_i \in \partial Q, \end{cases} \tag{10a}$$

$$v_i = \frac{\partial \mathcal{H}_{\text{agg}}}{\partial \theta_i}, \tag{10b}$$

where pr_Q is the orthogonal projection onto Q of the gradient vector given in Theorem III.3. For agents co-located with other agents at the same point p and associated Voronoi cell V, we define $S_i \subset \{+,-\}$ by specifying $s \in S_i$ if ∂w_i^s is not contained in the wedge of another agent located at p. Then, we set

$$u_i = 0, \tag{10c}$$

$$v_i = \sum_{s \in S_i} s \int_{V \cap \partial w_i^s} \|q - p_i\| f(\|q - p_i\|)\phi(q) dq. \tag{10d}$$

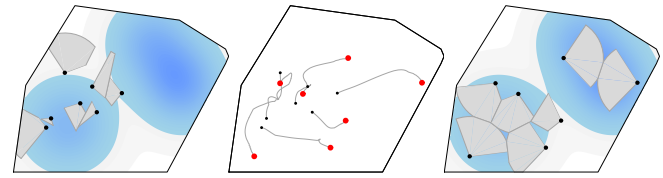

Fig. 3. Execution of the coordination algorithm (10) by 7 robots with sensory wedge radius $r = 0.345$ and $\alpha = \frac{\pi}{4}$. The plot on the left (resp. right) illustrates the initial (resp. final) configuration after 6.5 milliseconds. The central figure illustrates the gradient ascent flow of the system, with the smaller dots representing the initial configuration and the larger dots representing the final one. The performance function is $f(x) = 2 - x^2$ and the density function ϕ (represented by its contour plot) is the sum of three Gaussian functions of the form $50\, e^{-10((x-x_{\text{cntr}})^2 + (y-y_{\text{cntr}})^2)}$.

We assume that the Voronoi partition is updated in continuous time. The vector field is discontinuous, so we understand the solutions in the Krasovskii sense, see [11], [12].

Theorem IV.1 *Given a density function ϕ and a performance function f, the control law on $(Q \times \mathbb{S}^1)^n$ defined by* (10) *has the following properties:*

(i) *the law is spatially distributed over the limited-range Delaunay graph $\mathcal{G}_{LD}(\mathcal{P}, 2r)$ and;*

(ii) *for each initial configuration $(P_0, \Theta_0) \in (Q \times \mathbb{S}^1)^n$, the Krasovskii solution that exactly satisfies* (10) *monotonically optimizes $\mathcal{H}_{agg}$ and asymptotically converges to the union of $\mathcal{S}_{coinc}$ and the set of critical points of $\mathcal{H}_{agg}$.*

Proof: Statement (i) follows from the fact that, according to (8), the gradient of $\mathcal{H}_{\text{agg}}$ depends only on the position and orientation of p_i as well as those of its in- and out-neighbors in the (r,α)-limited wedge graph $\mathcal{G}_{\text{LW}}$, and, according to Lemma II.1, this graph is spatially distributed over $\mathcal{G}_{LD}$. Statement (ii) follows from considering the dynamical system defined by (10) on the compact and strongly invariant domain $(Q \times \mathbb{S}^1)^n$. The motion according to (10) of the nodes not co-located with any other node increases the value of $\mathcal{H}_{\text{agg}}$. Therefore, while the solution is outside $\mathcal{S}_{\text{coinc}}$, the function $\mathcal{H}_{\text{agg}}$ is monotonically optimized. If the solution does not reach $\mathcal{S}_{\text{coinc}}$, then the LaSalle Invariance Principle [13] guarantees that it will reach the set of critical points of $\mathcal{H}_{\text{agg}}$. Otherwise, the solution reaches $\mathcal{S}_{\text{coinc}}$ and stays in it. ■

A. Simulations

To illustrate the performance of the network under the coordination algorithm (10), we present some numerical simulations. The algorithm is implemented in Mathematica® as a main program running the simulation that makes use of a library of routines. The structure of this simulation is loosely described by the following procedure: first, the intersection of the bounded Voronoi cell V_i and the wedge $w_{r,\alpha}(p_i,\theta_i)$, for

$i \in \{1, \ldots, n\}$, is computed. Next, the r-limited Delaunay and (r, α)-limited wedge proximity graphs are constructed. Then, for each robot, information of its in- and out-neighbors is collected and used to construct the various parameterizations necessary for the gradient computation. Finally, the various surface and boundary integrals involved in the gradient of the locational optimization function $\mathcal{H}_{\text{agg}}$ are computed using the Mathematica® numerical integration routine `NIntegrate`. The position and orientation of each robot are then updated according to these results. Fig. 3 illustrates an execution.

V. Conclusions

We have introduced two locational optimization functions to measure the coverage of the environment provided by a group of robotic agents with limited-range anisotropic sensory. Based on considerations about the distributed computation of the gradient information, we have selected the aggregate expected-value function as our optimization criteria. We have characterized the smoothness properties of this objective function, computed its gradient, and characterized its spatially-distributed character. We have designed a gradient ascent strategy that is guaranteed to achieve optimal network deployment. Further research will include the analysis on the computational complexity of the current algorithm, the design of coordination algorithms implemented in discrete time, the synthesis of cooperative strategies to attain global optima of the aggregate objective function, and the study of similar deployment problems in nonconvex environments.

Acknowledgments

This research was partially supported by NSF CAREER award ECS-0546871.

References

[1] A. Okabe, B. Boots, K. Sugihara, and S. N. Chiu, *Spatial Tessellations: Concepts and Applications of Voronoi Diagrams*, 2nd ed., ser. Wiley Series in Probability and Statistics. New York: John Wiley, 2000.

[2] Q. Du, V. Faber, and M. Gunzburger, "Centroidal Voronoi tessellations: Applications and algorithms," *SIAM Review*, vol. 41, no. 4, pp. 637–676, 1999.

[3] Z. Drezner, Ed., *Facility Location: A Survey of Applications and Methods*, ser. Springer Series in Operations Research. New York: Springer Verlag, 1995.

[4] J. Cortés, S. Martínez, T. Karatas, and F. Bullo, "Coverage control for mobile sensing networks," *IEEE Transactions on Robotics and Automation*, vol. 20, no. 2, pp. 243–255, 2004.

[5] J. Cortés, S. Martínez, and F. Bullo, "Spatially-distributed coverage optimization and control with limited-range interactions," *ESAIM. Control, Optimisation & Calculus of Variations*, vol. 11, pp. 691–719, 2005.

[6] A. Howard, M. J. Matarić, and G. S. Sukhatme, "Mobile sensor network deployment using potential fields: A distributed scalable solution to the area coverage problem," in *International Conference on Distributed Autonomous Robotic Systems (DARS02)*, Fukuoka, Japan, June 2002, pp. 299–308.

[7] I. I. Hussein and D. M. Stipanovic̀, "Effective coverage control for mobile sensor networks with guaranteed collision avoidance," *IEEE Transactions on Control Systems Technology*, vol. 15, no. 4, pp. 642–657, 2007.

[8] A. Arsie and E. Frazzoli, "Efficient routing of multiple vehicles with no communications," *International Journal on Robust and Nonlinear Control*, 2007, to appear.

[9] A. Kwok and S. Martínez, "Energy-balancing cooperative strategies for sensor deployment," in *IEEE Conf. on Decision and Control*, New Orleans, LA, 2007, to appear.

[10] J. W. Jaromczyk and G. T. Toussaint, "Relative neighborhood graphs and their relatives," *Proceedings of the IEEE*, vol. 80, no. 9, pp. 1502–1517, 1992.

[11] N. N. Krasovskii, *Stability of motion. Applications of Lyapunov's second method to differential systems and equations with delay*. Stanford, CA: Stanford University Press, 1963, translated from Russian by J. L. Brenner.

[12] A. F. Filippov, *Differential Equations with Discontinuous Righthand Sides*, ser. Mathematics and Its Applications. Dordrecht, The Netherlands: Kluwer Academic Publishers, 1988, vol. 18.

[13] H. K. Khalil, *Nonlinear Systems*, 3rd ed. Englewood Cliffs, NJ: Prentice Hall, 2002.

Appendix A
A generalized conservation of mass law

A set $\Omega \subset \mathbb{R}^2$ is said to be *piecewise smooth* if its boundary, $\partial\Omega$, is a simple closed curve that admits a continuous and piecewise smooth (i.e. piecewise continuously differentiable) parameterization $\gamma : \mathbb{S}^1 \to \mathbb{R}^2$. Likewise, a collection of sets $\{\Omega(x) \subset \mathbb{R}^2 \mid x \in (a, b)\}$ is said to be a *piecewise smooth family* if $\Omega(x)$ is piecewise smooth for all $x \in (a, b)$, and there exists a continuous function $\gamma : \mathbb{S}^1 \times (a, b) \to \mathbb{R}^2$, $(\theta, x) \mapsto \gamma(\theta, x)$, continuously differentiable with respect to its second argument such that for each $x \in (a, b)$, the map $\theta \mapsto \gamma_x(\theta) = \gamma(\theta, x)$ is a continuous and piecewise smooth parameterization of $\partial\Omega(x)$. We refer to γ as a *parameterization for the family* $\{\Omega(x) \subset \mathbb{R}^2 \mid x \in (a, b)\}$.

The following result, originally stated and proved in [5], is an extension of the integral form of the Conservation-of-Mass law in fluid mechanics.

Proposition A.1 *Let $\{\Omega(x) \subset \mathbb{R}^2 \mid x \in (a, b)\}$ be a piecewise-smooth family of curves such that $\Omega(x)$ is strictly star-shaped for all $x \in (a, b)$. Let the function $\varphi : \mathbb{R}^2 \times (a, b) \to \mathbb{R}$ be continuous on $\mathbb{R}^2 \times (a, b)$, continuously differentiable with respect to its second argument for all $x \in (a, b)$ and almost all $q \in \Omega(x)$, and such that for each $x \in (a, b)$, the maps $q \mapsto \varphi(q, x)$ and $q \mapsto \frac{\partial\varphi}{\partial x}(q, x)$ are measurable, and integrable on $\Omega(x)$. Then, the function*

$$(a, b) \ni x \mapsto \int_{\Omega(x)} \varphi(q, x) dq$$

is continuously differentiable and

$$\frac{d}{dx} \int_{\Omega(x)} \varphi(q, x) dq = \int_{\Omega(x)} \frac{\partial\varphi}{\partial x}(q, x) dq + \int_{\partial\Omega(x)} \varphi(\gamma, x) n^t(\gamma) \frac{\partial\gamma}{\partial x} d\gamma, \tag{11}$$

where $n : \partial\Omega(x) \to \mathbb{R}^2$, $q \mapsto n(q)$, denotes the unit outward normal to $\partial\Omega(x)$ at $q \in \partial\Omega(x)$, and $\gamma : \mathbb{S}^1 \times (a, b) \to \mathbb{R}^2$ is a parametrization for the family $\{\Omega(x) \subset \mathbb{R}^2 \mid x \in (a, b)\}$.